Journal of Electrotechnology, Electrical Engineering and Management (2024) DOI: 10.23977/jeeem.2024.070105
Clausius Scientific Press, Canada ISSN 2560-6697 Vol. 7 Num. 1

Fault Diagnosis of Sensors for Multi-stack Fuel Cell Thermal Management Subsystem Based on UKF

Zhou Su[1,a], Jiang Yongyuan[1,b,*], Gao Jianhua[1,c]

[1]College of Automotive Studies, Tongji University, Shanghai, 201804, China
[a]suzhou@tongji.edu.cn, [b]2133570@tongji.edu.cn, [c]2011692@tongji.edu.cn
[*]Corresponding author

Keywords: Multi-stack fuel cell, Thermal management subsystem, Unscented Kalman Filter, Fault diagnosis, Difference calculation

Abstract: In Multi-stack fuel cell system (MFCS), the thermal management subsystem has various heat dissipation structures and heat dissipation forms, and the stability and accuracy of its operation are important indicators to ensure the safety of the system. In this paper, a water-cooled integrated MFCS thermal management subsystem model is established, and a sensor fault diagnosis method based on Unscented Kalman Filter (UKF) is proposed for the sensor fault in the thermal management subsystem, which adopts the Unscented Transform for the nonlinear system and obtains the estimated value through three processes of prediction, update and iterative calculation. The difference calculation method is adopted to calculate the fused residuals of the UKF estimates and the measured values of the thermal management subsystem sensors to obtain fault information for single or multiple sensors. The results show that the fault diagnosis using the difference method of UKF estimate and the sensor measurements residual signal for the variation of MFCS thermal management subsystem structure and signal acquisition can quickly determine the type and location of single or multiple sensor faults in the thermal management subsystem.

1. Introduction

With the development of new energy technologies, the energy structure has also undergone great changes, and in the field of transportation, the power of various modes of transportation has also shifted from the traditional fossil fuel power source to various new and renewable energy power sources [1,2]. Proton exchange membrane fuel cell (PEMFC), which is fueled with clean energy hydrogen, is a very representative power source equipment, which not only has the similar fast refueling method and power delivery method of traditional internal combustion engine, but also has the advantages of low operating temperature, high power density, low noise and no pollution, which can be expanded and developed on the basis of existing transportation tools [3].

To meet the demand power of transportation tools and electromechanical engineering equipment in various application scenarios, the current capacity of single-stack fuel cell system is obviously insufficient, and high-power multi-stack fuel cell system (MFCS) is a better solution for the current stage. MFCS does not require a large amount of research investment for the development of high-power single-stack fuel cell system, and can also prevent the continuous damage of the stacks by fault isolation and switching operation when a single stack fails, which can satisfy the requirements of high-power application scenarios by using the existing fuel cell technology [4,5].

For the above MFCS, the structure of the subsystem will change greatly according to the needs and applications of each power stack, and there are currently two types [6]: integrated and distributed. Compared with the distributed subsystem, the integrated subsystem integrates and redistributes the overlapping parts of the function, which reduces the cost of the system and improves the system integration, but it is more difficult to control and monitor, mainly because some of the signals measured by the setup sensors belong to the information shared by multiple systems, and the inconsistency of the demanded power of each power reactor also raises the difficulty of the subsystem's supply demand, which is a great challenge for both the controller and the monitoring of the operating status of the system [7]. For the thermal management subsystem (TMS), the cooling method and the circulation structure of the cooling loop have different impacts on the maintenance of the operating temperature and energy consumption of each stack the MFCS, and the TMS directly determines the operating temperature of the electrochemical reaction inside the fuel cell through various forms of cooling circulation methods. The operating temperature of the fuel cell has a great impact on typical faults such as water flooding and membrane drying, and ensuring the stable operation of the TMS is a necessary prerequisite to ensure the normal operation of the fuel cell [8,9]. So far, in the research of TMS, most scholars are concerned about the impact on the fuel cell performance and auxiliary equipment components, for the structure of the TMS, control methods and fault diagnosis there have been a lot of research results, and the research on the sensor fault can be easily ignored [10], with the deepening of the research and the rapid development of the fuel cell technology, the problem of the sensor fault has also had some research advances. Mao et al [11] proposed an algorithm for sensor selection considering the sensitivity of sensors to various faults, which provides more efficient sensor selection results with less computation time. Yan et al [12] proposed the Dulmage-Mendelsohn decomposition method to design a residual generator for sensor faults in response to the problem of sensor faults in the thermal management system of the PEMFC,the experimental results show that the temperature of the stack follows the system setpoint well with high accuracy even if the sensor fails.

The sharing of sensor information in the MFCS integrated thermal management subsystem and the fact that multiple sensor faults can interact with each other make the sensor fault problem a serious impact on the operation and output performance of the MFCS. Therefore, in this paper, a sensor fault diagnosis method based on Unscented Kalman Filter (UKF) is proposed for the sensor fault problem in TMS. UKF uses the unscented transform to select Sigma sampling points and calculate the weights. The prediction process is carried out after the selection of the point set, the point set is brought into the nonlinear system function to get the state of the Sigma point set at the moment t, and the weighting calculation is carried out to get the a priori estimation of its mean and error covariance, and according to the a priori estimation and the mean and mean covariance of the observed values at the moment t, the Kalman filtering gain and a posteriori estimation are calculated. Iterative calculations are performed sequentially, and the difference fusion calculation is performed between the UKF estimate and the residual signals of sensor measurements in the TMS, and the difference residual signals are utilized to obtain information about single or multiple sensor faults, and to carry out diagnosis and localization of sensor faults.

2. Description of the TMS and sensor fault in MFCS

The MFCS thermal management integrated subsystem mainly includes coolant storage tank, coolant circulating pump, bypass valve, intercooler, splitter, mixer, deionizer, thermostat, radiator, water replenisher, sensors, and circulating pipelines, as shown in Figure 1. According to the heat production during the electrochemical reaction of different stack (20kW, 70kW and 120kW) of the MFCS, the speed of the coolant circulation pump and the diverter opening are adjusted in real time to ensure that the working temperature of each stack is stable. The TMS constrains the temperature of the stack through forced convection heat transfer between the coolant and the stack, which requires various heat exchangers and power units to realize its function, and sensor information for monitoring and feedback.

Sensor fault, that is, for the current system needs to measure the value, the sensor can not get the real similar value and make the measurement information is not accurate. This kind of fault leads to a large error in the output value of the sensor, while the characteristics of the sensor measurement object does not change, these large errors in the output value is transmitted to other components or controllers, which will cause the system to have a larger error and make the system fail [13,14]. In the fuel cell thermal management subsystem, the main sensor is a temperature sensor, which is used to obtain the temperature information of the coolant in each functional section, so that the coolant circulating pump and the various valves and other actuators to take feedback adjustment to stabilize the temperature of the stack in a reasonable threshold range.

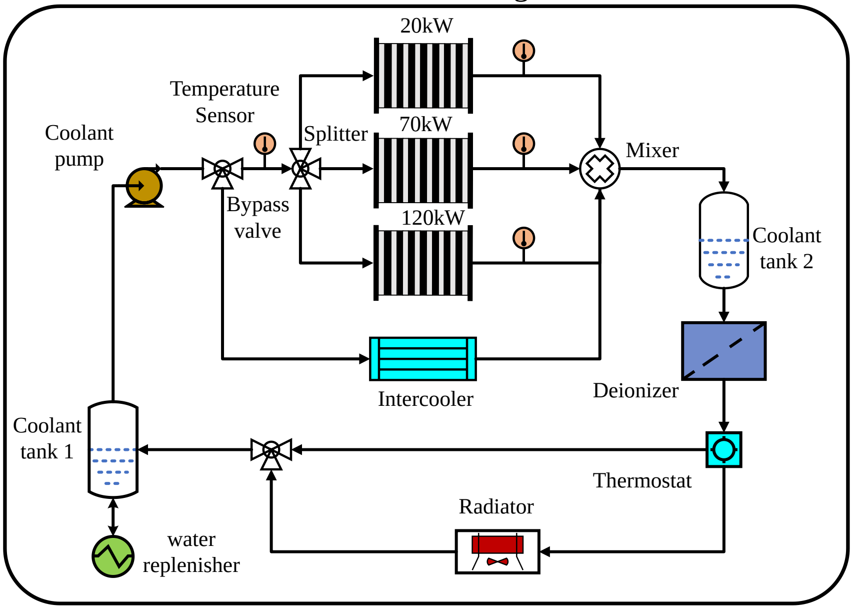

Figure 1: MFCS thermal management subsystem structure.

The true value of the output of the system is often not available, so it is necessary to measure the output value that needs to be obtained using a sensor, which can be expressed as:

$$y_m = y_r \cdot f_t + f_c + w \tag{1}$$

where, y_m is the measured sensor value, y_r is the actual system value, f_t is the multiplicative sensor fault, f_c is the additive sensor fault, w is the system noise.

The above fault types mainly include two types of faults, namely multiplicative fault and additive fault, also known as soft fault and hard fault. Multiplicative fault refers to a small difference between the sensor measurement value and the normal measurement value at a certain moment, which gradually increases over time, while additive fault refers to a significant error between the measured value of the sensor and the actual value due to a step at a certain moment.

3. Sensor fault diagnosis for the TMS of MFCS

3.1. Design of the UKF

The multi-stack fuel cell thermal management subsystem model has strong nonlinear characteristics, and the use of UKF does not need to linearize the nonlinear equations and solve the Jacobian matrix, which ensures better computational accuracy and also reduces the amount of computation and computation time. The core of the UKF is the unscented transformation, which first generates a set of Sigma points with the same statistical information as the desired transferred state variables, then transforms and transfers each Sigma point with a nonlinear function, and finally uses the transformed Sigma points to determine the statistical characteristics of the output values. In this paper, the symmetric sampling method is used and the unscented transformation is formulated as follows:

(1) Obtain a set of Sigma points,

$$\begin{cases} x_i = \bar{x}, i = 0 \\ x_i = \bar{x} + \left[\sqrt{(n+\lambda)P}\right]_i, i = 1\sim n \\ x_i = \bar{x} - \left[\sqrt{(n+\lambda)P}\right]_i, i = n+1\sim 2n \end{cases} \tag{2}$$

where, $\bar{x}$ is the average value of x; n is the dimension of the state variable x; P is the covariance; λ is the scaling factor;

(2) Calculate the weight of Sigma points,

$$\begin{cases} \omega_i^m = \lambda/(n+\lambda), i = 0 \\ \omega_i^c = \lambda/(n+\lambda) + (1-\alpha^2+\beta), i = 0 \\ \omega_i^m = \omega_i^c = 1/[2(n+\lambda)]_i, i = 1\sim 2n \end{cases} \tag{3}$$

where, ω_i^m and ω_i^c are respectively the average weighted coefficients and variance weighted coefficients of the *i-th* Sigma point, the distribution state of the sampling point can be controlled by adjusting α, with a value range of $e^{-1} < \alpha < 1$, β is a non-negative weighting coefficient, which is used to reduce the error of the higher-order terms, and β is often taken as the value of 2 when the process noise and the measurement noise obey the Gaussian distribution.

(3) Nonlinear transformations and transfers of Sigma point set

$$y_i = f(x_i), i = 1\sim 2n \tag{4}$$

(4) Determine the output value,

$$\begin{cases} \bar{y} = \sum_{i=0}^{2n} \omega_i^m y_i \\ P_{yy} = \sum_{i=0}^{2n} \omega_i^c (y_i - \bar{y})(y_i - \bar{y})^T \end{cases} \tag{5}$$

According to the established model of the multi-stack fuel cell thermal management subsystem, the system parameter variables for parameter estimation using UKF are determined as the inlet coolant temperature and the outlet coolant temperatures of the three stacks, the disturbances are the ambient temperatures and the demand currents of the three stacks, and the sensor measurement parameters are the inlet coolant temperature, and the temperatures of the three stacks. Assuming that the temperature of the stacks is equal to the outlet coolant temperature, then the state variables of the system are the same as the observed variables, and the thermal management subsystem of the multi-stack fuel cell can be described as:

$$\begin{cases} x_t = f(x_{t-1}, u_{t-1}) + w_t \\ y_t = h(x_t, u_t) + v_t \end{cases} \tag{6}$$

where, x is the state variable, $x = [x_1, x_2, x_3, x_4, x_5, x_6]^T$, x_1, x_2 and x_3 are respectively the coolant outlet temperatures of stack 1, 2 and 3, x_4 is the coolant inlet temperature of the stack, x_5 is the coolant outlet temperature of the radiator, x_6 is the coolant inlet temperature of the radiator; u is the input variable, $u = [u_1, u_2, u_3, u_4, u_5, u_6]^T$, u_1 is the coolant circulating pump rotational speed, u_2 is the thermostat opening, u_3 is the radiator fan rotational speed, u_4 is the bypass valve opening, u_5 is the throttle opening into stack 1, u_6 is the throttle opening into stack 2; y is the output variable, $y = [y_1, y_2, y_3, y_4]^T$, y_1, y_2 and y_3 are respectively the coolant outlet temperatures of stacks 1, 2 and 3, y_4 is the coolant inlet temperature; w_t and v_t are the system noises. The state-space equations of the integrated thermal management subsystem of the MFCS are:

$$\begin{vmatrix} \hat{x}_1(t+1) \\ \hat{x}_2(t+1) \\ \hat{x}_3(t+1) \\ \hat{x}_4(t+1) \\ \hat{x}_5(t+1) \\ \hat{x}_6(t+1) \end{vmatrix} = \begin{vmatrix} a_{1,1} & 0 & 0 & a_{1,4} & 0 & 0 \\ 0 & a_{2,2} & 0 & a_{2,4} & 0 & 0 \\ 0 & 0 & a_{3,3} & a_{3,4} & 0 & 0 \\ 0 & 0 & 0 & a_{4,4} & a_{4,5} & a_{4,6} \\ 0 & 0 & 0 & 0 & a_{5,5} & a_{5,6} \\ a_{6,1} & a_{6,2} & a_{6,3} & 0 & 0 & 0 \end{vmatrix} \begin{vmatrix} \hat{x}_1(t) \\ \hat{x}_2(t) \\ \hat{x}_3(t) \\ \hat{x}_4(t) \\ \hat{x}_5(t) \\ \hat{x}_6(t) \end{vmatrix} + \begin{vmatrix} b_1(t) \\ b_2(t) \\ b_3(t) \\ b_4(t) \\ b_5(t) \\ b_6(t) \end{vmatrix} \tag{7}$$

where, $\hat{x}_i$ is the state bias, the coefficients of the system state space are determined from the actuator parameters and operating conditions in the TMS.

The iterative computation process of the UKF algorithm incorporates the unscented transformation, and its algorithmic flow is shown in Figure 2. Firstly, the system state variables and their error covariances are initialized $\hat{x}_0 = E(x_0), P_0 = [(x_0 - \hat{x}_0)(x_0 - \hat{x}_0)]$, and the Sigma sampling points are selected and weights are calculated according to Equation (2) and (3). Then the selected point set is brought into the nonlinear system function to obtain the state of the Sigma point set at the moment *t* and weighted to obtain the prior estimates of its average value and error covariance. Finally, based on the prior estimate, the average value and the mean variance of the observations at the moment *t*, the Kalman filter gain and the posterior estimate are computed, and the iterative computation is carried out sequentially.

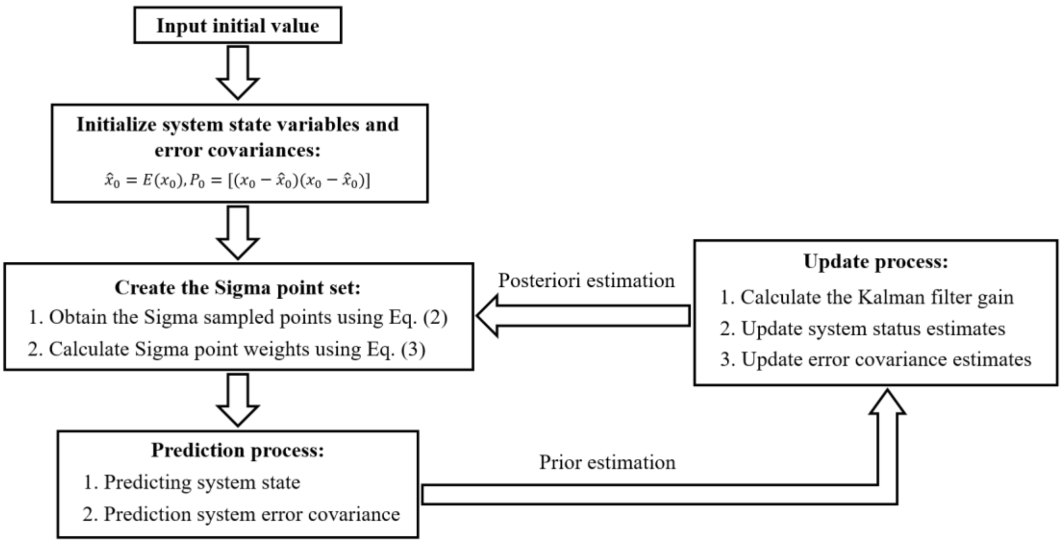

Figure 2: Flowchart of UKF algorithm.

3.2. Sensor fault diagnosis based on UKF

The previously described UKF is used to design the temperature observer by predicting each state variable of the MFCS integrated thermal management subsystem, which is applied to the UKF for a priori estimation of the state variables of the system, and determining whether the temperature sensor is malfunctioning or not by comparing the residuals between the measured values of the temperature sensors in the model of the MFCS integrated thermal management subsystem and the estimated values. A single sensor fault only requires comparing the residuals between the measured and estimated values of a single temperature sensor, while a multiple sensor fault requires identifying the faulty sensor based on the characteristics of the residuals of multiple sensors, and then carrying out fault type identification and fault isolation. If the number of variable signals that the TMS needs to be measured by the sensors is *m*, *m* UKFs need to be designed to obtain the sensor residual signals. Sensor fault identification and localization can be performed by differential fusion calculation of residual signals using (*m-n*) sensor residual signals, where *n* is the difference value, *n* = 0, 1, 2, 3, ... (*m-1*). The fusion residual for a difference of 1 is calculated as in Equation (8).

$$RMSE_j = \sqrt{\frac{1}{m-1}\left[\sum_{k=1}^{m}(y_k - \hat{y}_k)^2 - \left(y_j - \hat{y}_j\right)^2\right]} \tag{8}$$

where, $RMSE_j$ is the fusion residual of *j-th* sensor.

The sensors diagnosed in this paper include the stack inlet coolant temperature sensor and three stack outlet coolant temperature sensors. The MFCS integrated thermal management subsystem sensor fault diagnosis and isolation process is shown in Figure 3.

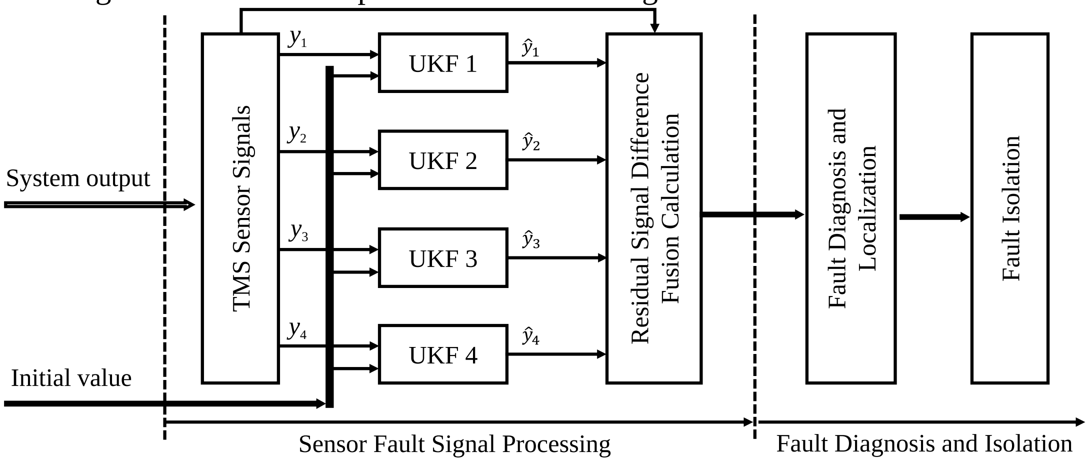

Figure 3: Structure of sensor fault diagnosis of TMS based on UKF.

4. Sensor fault localization and fault identification results

The established TMS model is fed with certain signals to get the output values measured by the sensors, and the four sensors of the TMS are labeled as S1, S2, S3 and S4 (20kW stack outlet temperature sensor, 70kW stack outlet temperature sensor, 120kW stack outlet temperature sensor and inlet temperature sensor) for fault indication. According to the sensor fault characteristics, each fault is added at a certain moment, the sensor faults are classified according to the UKF, and the filtered residual signal is obtained for difference fusion calculation, and then the fault localization and diagnosis are carried out according to the signal logic judgment.

Figure 4 shows the variation of fusion residuals of different sensors when the difference is 1 under S2 fault (hard fault of S2 sensor is set at 250s of system runtime). As shown in Figure 4, (a), (b), (c) and (d) correspond to the fusion residuals of four sensors (S4, S3, S2 and S1) of the TMS, and the fusion residual signal value in Figure 4(c) is small and basically stable, which indicates that its corresponding sensor, S2, has failed. The fused residuals in the other figures are stabilized at a certain value after an offset occurs, so it can be determined that the type of fault is a hard fault, which is consistent with the setup fault. Combined with the calculation of each fusion residual and logical judgment, it can be determined that a hard fault occurs in S2 at 250s of system runtime (i.e. setup time of the fault).

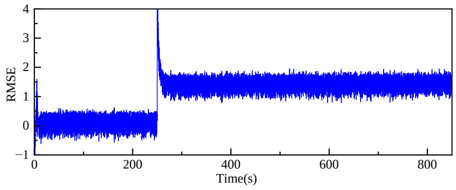

(a) Fused residuals of S1, S2, S3

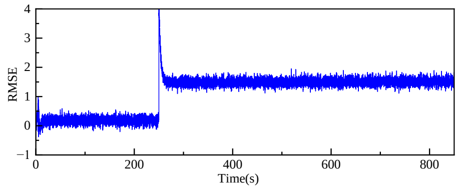

(b) Fused residuals of S1, S2, S4

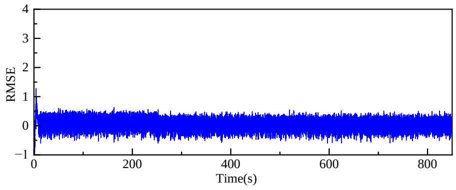

(c) Fused residuals of S1, S3, S4

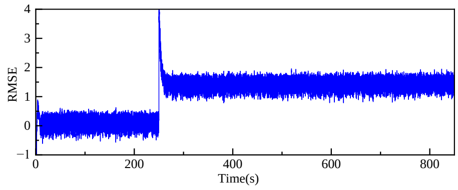

(d) Fused residuals of S2, S3, S4

Figure 4: Fused residual curves with hard fault of S2 sensor.

Figure 5 shows the variation of fusion residuals of different sensors when the difference is 1 under the S2 fault (a mixed fault of soft and hard fault is set at 250s of system runtime). Figure 5(a), (b), (c) and (d) correspond to the fusion residuals of the four sensors of the TMS (S4, S3, S2 and S1), respectively, and the fusion residual signal value of Figure 5(c) is very small and does not have a large change, indicating that its corresponding sensor S2 has failed. The fusion residuals in the other figures continue to drift over time after the offset occurs, from which it can be determined that both hard and soft faults occur in S2, i.e. a mixed fault occurs. Combined with the calculation and logical judgment of each fusion residual, it can be determined that a mixed fault occurs in S2 at 250s (i.e. setup time of the fault) of the system operation. In addition, compared with Figure 4(c), the signal of the fusion residuals in Figure 5(c) decreases slightly with time, indicating that the continuous drift will have a certain impact on the calculation results of the fusion residuals, which will affect the accuracy of the fault discrimination.

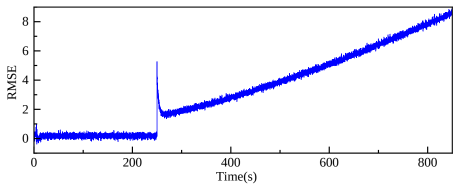

(a) Fused residuals of S1, S2, S3

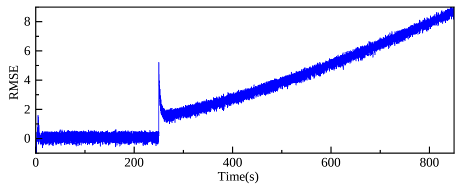

(b) Fused residuals of S1, S2, S4

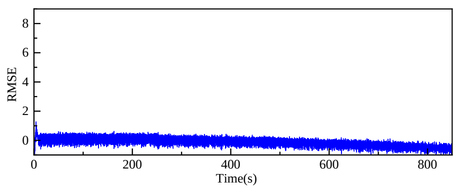

(c) Fused residuals of S1, S3, S4

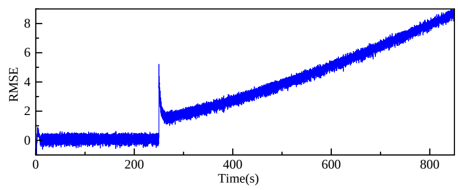

(d) Fused residuals of S2, S3, S4

Figure 5: Fused residual curves with mixed fault of S2 sensor.

The residuals calculated by fusion when the difference is 1 cannot be used for fault judgment of the signals when multiple sensors are faulty, so it is necessary to increase the value of the difference, and the diagnosis and localization when 2 sensors are faulty can be satisfied when the difference is 2. Figure 6 shows the change of fused residual signals of different sensors when the difference is 2 under the S2 and S3 faults (S2 is set up for mixed faults when the system running time is 250s, and S3 is set up for hard faults when the system running time is 120s). The fused residual signal values in Figure 6(c) are small and do not change significantly, so it can be determined that the S2 and S3 sensors are faulty. Combined with the other fusion residual offset times and offset changes in Figure 6, it can be determined that a mixed fault occurs in S2 at 250s of system operation (i.e. S2 sensor fault setup time), and a hard fault occurs in S3 at 120s of system operation (i.e. S3 sensor fault injection time), i.e. more than one sensor faults occur in the TMS.

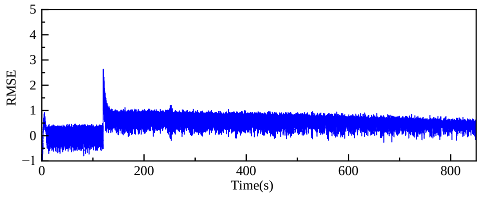

(a) Fused residuals of S1, S2

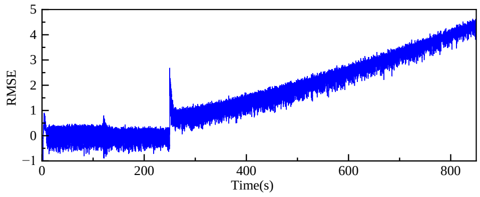

(b) Fused residuals of S1, S3

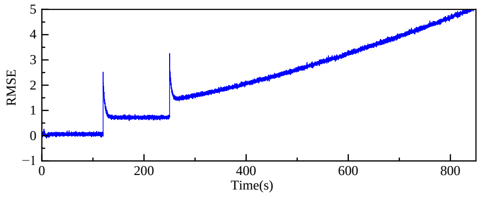

(c) Fused residuals of S1, S4

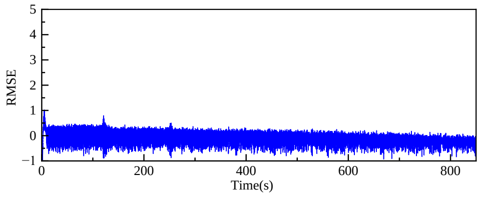

(d) Fused residuals of S2, S3

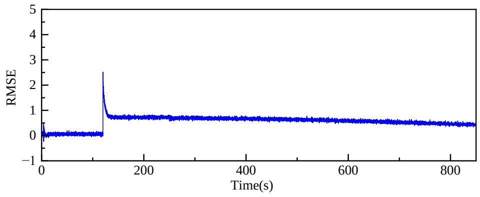

(e) Fused residuals of S2, S4

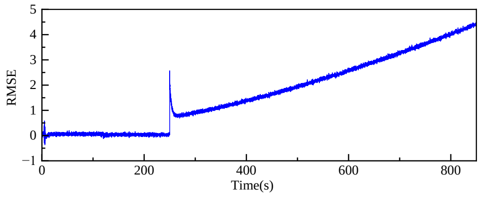

(f) Fused residuals of S3, S4

Figure 6: Fused residual curves with mixed fault of S2 sensor and hard fault of S3 sensor.

5. Conclusions

In this paper, an integrated MFCS thermal management subsystem model is established, and a UKF-based sensor fault diagnosis method is proposed for sensor fault problems occurring in the system, which performs difference fusion calculation of the residual signals between the UKF estimates and the sensor measurements in the TMS to obtain single or multiple sensor fault information. The results show that for the changes in the structure and signal acquisition of the integrated thermal management subsystem of the MFCS, the fault diagnosis using the UKF and sensor difference signal processing method is able to quickly diagnose the type and location of single or multiple sensor faults in the TMS based on the fused residual offsets and the change of the offsets over time.

References

[1] Kwilinski A, Lyulyov O, Pimonenko T. Reducing transport sector CO2 emissions patterns: Environmental

technologies and renewable energy [J]. Journal of Open Innovation: Technology, Market, and Complexity, 2024, 10(1): 100217.
[2] Lindstad E, Ask T Ø, Cariou P, et al. Wise use of renewable energy in transport [J]. Transportation Research Part D: Transport and Environment, 2023, 119: 103713.
[3] JIAO Kui, XUAN Jin, DU Qing, et al. Designing the next generation of proton-exchange membrane fuel cells [J]. Nature, 2021, 361-369.
[4] Cullen D A, Neyerlin K C, Ahluwalia R K, et al. New roads and challenges for fuel cells in heavy-duty transportation [J]. Nature Energy, 2021, 462-474.
[5] Zhang G, Zhou S, Gao J, et al. Stacks multi-objective allocation optimization for multi-stack fuel cell systems[J]. Applied Energy, 2023, 331: 120370.
[6] Mehida H, Ayad M Y, Saadi R, et al. Multi-stack fuel cells and interleaved DC/DC converters interactions for embedded applications[C]//2018 International Conference on Electrical Sciences and Technologies in Maghreb (CISTEM). IEEE, 2018: 1-6.
[7] Zhou Su, Fan Lei, Zhang Gang, et al. A review on proton exchange membrane multi-stack fuel cell systems: architecture, performance, and power management [J]. Applied Energy, 2022, 310:118555.
[8] Li Yuehua, Yang Fan, Chen Dongfang, et al. Thermal-physical modeling and parameter identification method for dynamic model with unmeasurable state in 10-kW scale proton exchange membrane fuel cell system[J]. Energy Conversion and Management, 2023, 276:116580.
[9] Dépature C, Boulon L, Sicard P, et al. Simulation model of a multi-stack fuel cell system[C]//2013 15th European Conference on Power Electronics and Applications (EPE). IEEE, 2013: 1-10.
[10] Dijoux E, Steiner N Y, Benne M, et al. A review of fault tolerant control strategies applied to proton exchange membrane fuel cell systems [J]. Journal of Power Sources, 2017, 359(aug.15):119-133.
[11] Mao Lei, Jackson L, Davies B. Effectiveness of a novel sensor selection algorithm in PEM fuel cell on-line diagnosis [J]. IEEE Transactions on Industrial Electronics, 2018:1-1.
[12] Yan Chizhou, Chen Jian, Liu Hao, et al. Model-based Fault Tolerant Control for the Thermal Management of PEMFC Systems [J]. IEEE Transactions on Industrial Electronics, 2019, PP (99):1-1.
[13] Shen D, Yang D, Lyu C, et al. Multi-sensor multi-mode fault diagnosis for lithium-ion battery packs with time series and discriminative features [J]. Energy, 2024, 290: 130151.
[14] Jihani N, Kabbaj M N, Benbrahim M. Kalman filter based sensor fault detection in wireless sensor network for smart irrigation [J]. Results in Engineering, 2023, 20: 101395.